Supplementary Information

Room temperature multiferroicity in $Bi_{4.2}K_{0.8}Fe_2O_{9+\delta}$

Si-Ning Dong[1], Yi-Ping Yao[1], Jian-Qi Li[2], Yuan-Jun Song[2], Yu-Kuai Liu[1], and Xiao-Guang Li[1,*]
[1]Hefei National Laboratory for Physical Sciences at Microscale, Department of Physics, CAS Key Lab Mat Energy Convers, University of Science and Technology of China (USTC), Hefei 230026, P. R. China
[2]Beijing National Laboratory for Condensed Matter Physics, Institute of Physics, Academia Sinica, Beijing 100190, P. R. China
[*]To whom correspondence should be addressed. E-mail: lixg@ustc.edu.cn

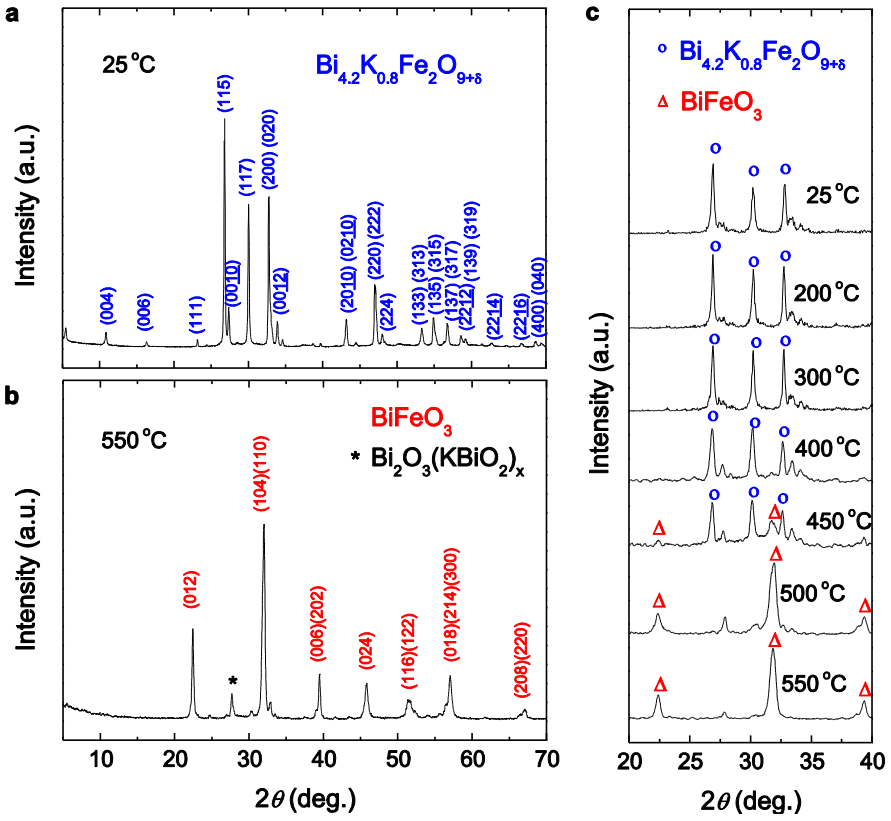

Supplementary Fig. S1| **a**, X-ray diffraction patterns ($5^o \le 2\theta \le 70^o$) of the $Bi_{4.2}K_{0.8}Fe_2O_{9+\delta}$ nanobelts at 25 °C; **b**, for the sample at 550 °C, which is mainly decomposed to $BiFeO_3$ with a $Bi_2O_3(KBiO_2)_x$ impurity phase (marked by asterisks); and **c**, X-ray diffraction patterns ($20^o \le 2\theta \le 40^o$) for the sample at different temperatures (the stronge diffraction peaks of $Bi_{4.2}K_{0.8}Fe_2O_{9+\delta}$ are marked with open blue circles and those of $BiFeO_3$ are marked with open red triangles). The results demonstrate that the $Bi_{4.2}K_{0.8}Fe_2O_{9+\delta}$ nanobelts will be decomposed above 450 °C. Therefore, the thermal instability of the $Bi_{4.2}K_{0.8}Fe_2O_{9+\delta}$ makes it a difficulty to obtain the corresponding bulk materials (big single crystal or dense ceramic) through a conventional solid state reaction method so far.

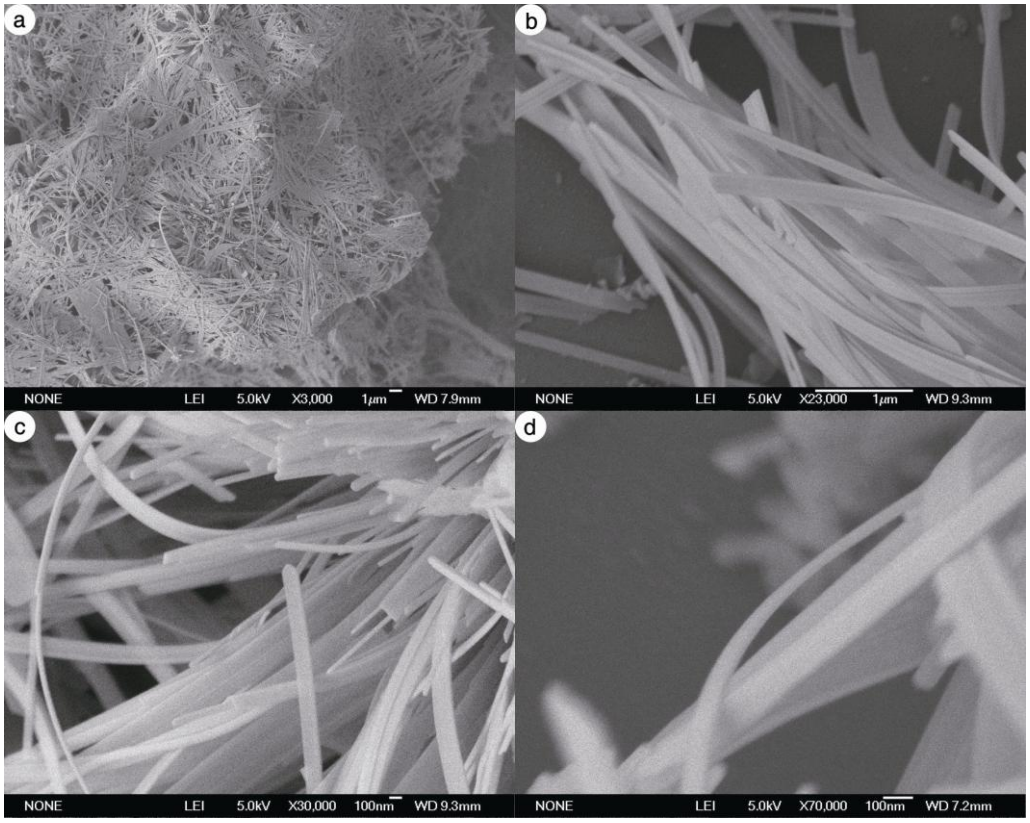

Supplementary Fig. S2| Scanning electron microscopy (SEM) images of the $Bi_{4.2}K_{0.8}Fe_2O_{9+\delta}$ nanobelts with different magnification.

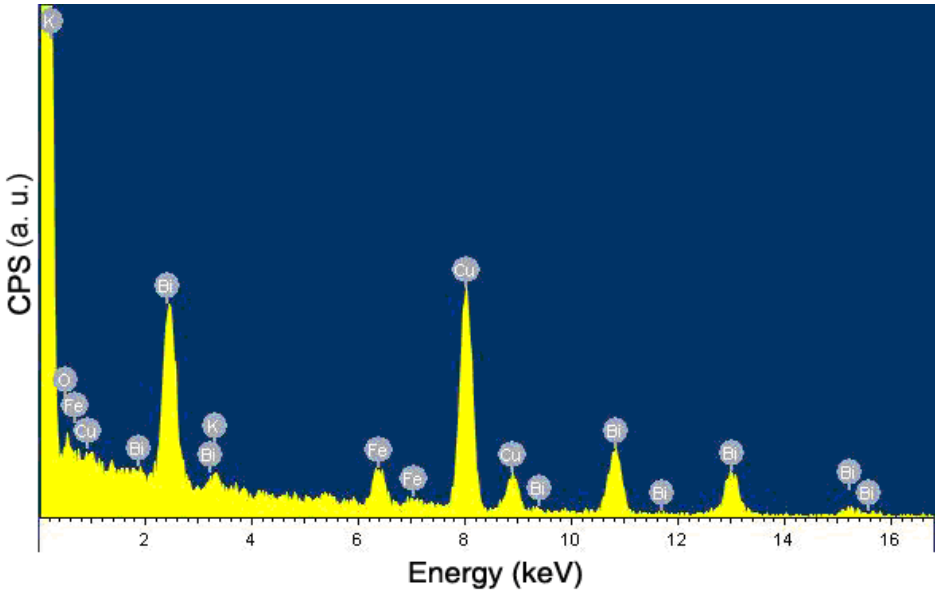

Supplementary Fig. S3| Energy-dispersive X-ray spectrometry (EDS) of the $Bi_{4.2}K_{0.8}Fe_2O_{9+\delta}$ nanobelts. For the measurement the nanobelts are dispersed on the copper grids.

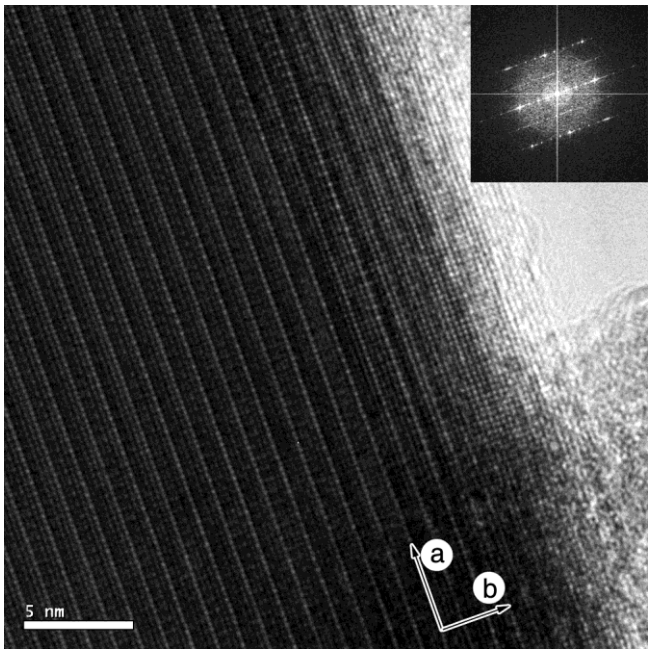

Supplementary Fig. S4| High-resolution transmission electron microscopy (HRTEM) image of the edge of a single nanobelt, the inset is the Fourier transform of the HRTEM image.

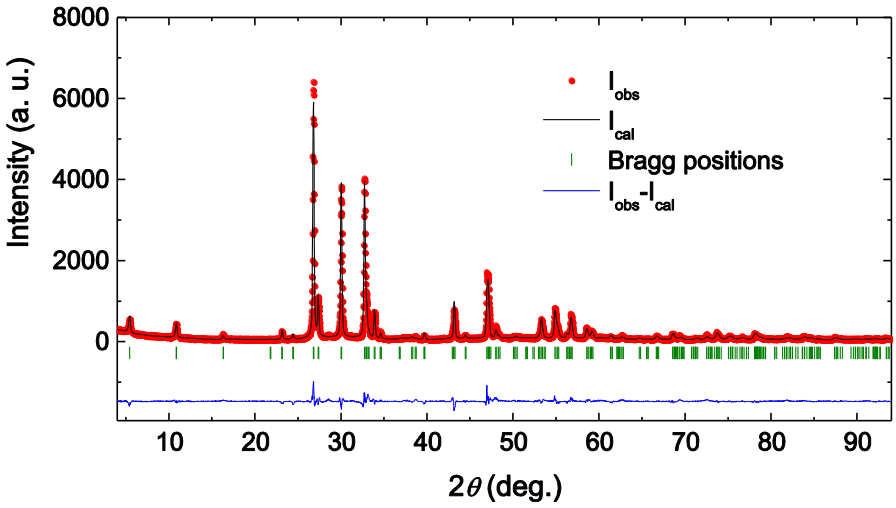

Supplementary Fig. S5| Preliminary Rietveld refinements for the powder XRD patterns ($4^{o} \leq 2\theta \leq 94^{o}$) of the $Bi_{4.2}K_{0.8}Fe_2O_{9+\delta}$ nanobelts using the Fullprof software (Ref: Rodriguez-carvajal, J. Recent Advances in Magnetic-Structure Determination by Neutron Powder Diffraction. *Physica B* **192**, 55-69 (1993)). The refinements are started with the space group ***F***mmm without considering the modulated structure and the final conventional Rietveld *R*-factors (without the deduction of the background signal) are: R_p = 18.4, R_{wp} = 19.2 and R_{exp} = 13.04. The calculated results agree with the experimental diffraction patterns. Moreover, the refinements have confirmed that the K atoms occupy some of the Bi sites in the perovskite layers not the rock salt layers.

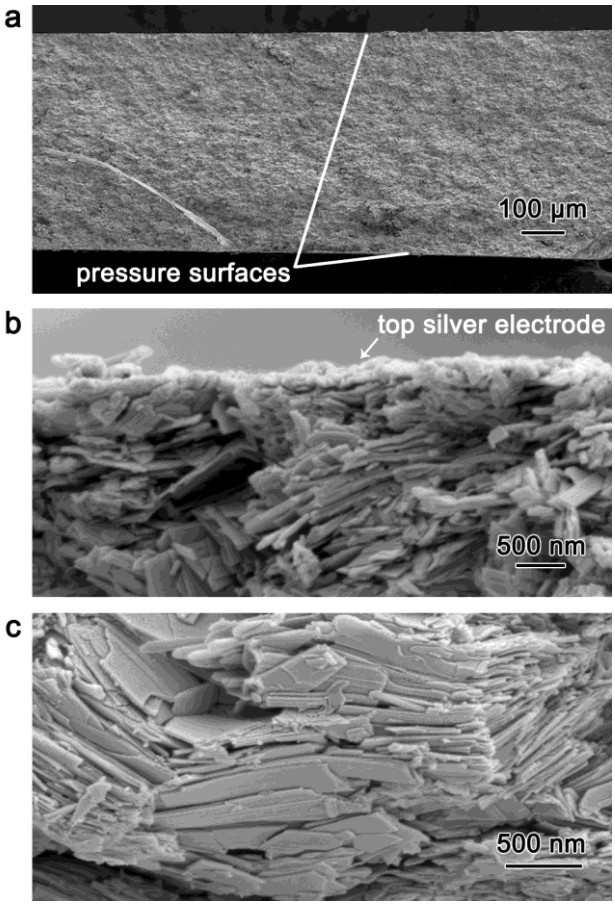

Supplementary Fig. S6| SEM images of the cross-section of a $Bi_{4.2}K_{0.8}Fe_2O_{9+\delta}$ bulk for the electric measurements. **a**, low-magnification view; **b** and **c**, high-magnification images taken at the top surface and center regions of the bulk, respectively, without rotating the sample direction. One can see a large amount of nanobelts with the ***c***-axes perpendicular to the pressure surface, some nanobelts with the ***b***-axes perpendicular to the pressure surface, and other intermediately oriented nanobelts.

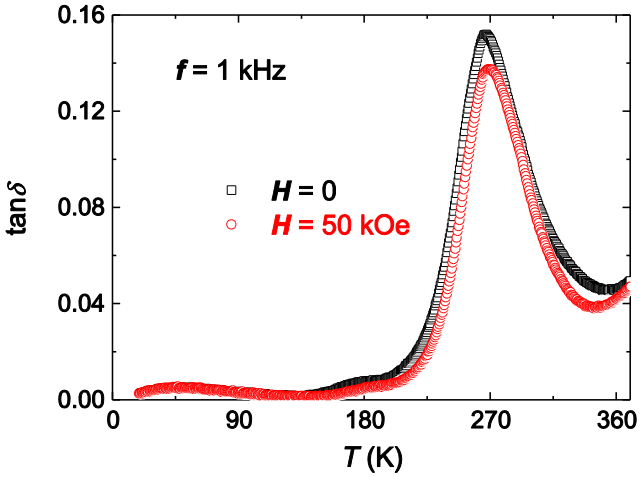

Supplementary Fig. S7| Temperature dependencies of dielectric loss tanδ of the bulks made of the $Bi_{4.2}K_{0.8}Fe_2O_{9+\delta}$ nanobelts at 1 kHz under zero (black open square) and 50 kOe (red open circle) magnetic fields, respectively.